Chapter 7
Printing Processes

Printing technology has been extensively investigated, with the majority of that investigation historically based upon applications to the two-dimensional printing industry. Recently, however, it has spread to numerous new application areas, including electronics packaging, optics, and additive manufacturing. Some of these applications, in fact, have literally taken the technology into a new dimension. The employment of printing technologies in the creation of three-dimensional products has quickly become an extremely promising manufacturing practice, both widely studied and increasingly widely used.

This chapter will summarize the printing achievements made in the additive manufacturing industry and in academia. The development of printing as a process to fabricate 3D parts is summarized, followed by a survey of commercial polymer printing machines. Both direct part printing and binder printing technologies are introduced. Direct printing refers to processes where all of the part material is dispensed from a print head, while binder printing refers to a broad class of processes where binder or other additive is printed onto a powder bed which forms the bulk of the part. Some of the technical challenges of printing are introduced; material development for printing polymers, metals, and ceramics is investigated in some detail. From the topic of pure printing technologies, we move to the three-dimensional binder printing process, where binder is printed into a powder bed to form a part.

7.1 Evolution of Printing as an Additive Manufacturing Process

Two-dimensional inkjet printing has been in existence since the 1960s, used for decades as a method of printing documents and images from computers and other digital devices. Inkjet printing is now widely used in the desktop printing industry, commercialized by companies such as HP and Canon. Le [1] provides a thorough review of the historical development of the inkjet printing industry.

I. Gibson, D.W. Rosen, and B. Stucker, *Additive Manufacturing Technologies*,
DOI 10.1007/978-1-4419-1120-9_7,

7.1.1 Historical Development of 3D Printing

Printing as a three-dimensional building method was first demonstrated in the 1980s with patents related to the development of Ballistic Particle Manufacturing, which involved simple deposition of "particles" of material onto an article [2]. The first commercially successful technology was the ModelMaker from Sanders Prototype (now Solidscape), introduced in 1994, which printed a basic wax material that was heated to liquid state [3]. In 1996, 3D Systems joined the competition with the introduction of the Actua 2100, another wax-based printing machine. The Actua was revised in 1999 and marketed as the ThermoJet [3]. In 2001, Sanders Design International briefly entered the market with its Rapid ToolMaker, but was quickly restrained due to intellectual property conflicts with Solidscape [3]. It is notable that all of these members of the first generation of RP printing machines relied on heated waxy thermoplastics as their build material; they are therefore most appropriate for concept modeling and investment casting patterns.

Binder printing methods were developed in the early 1990s, primarily at MIT. They developed the 3D Printing (3DP) process in which a binder is printed onto a powder bed to form part cross sections. Contrast this concept with SLS, where a laser melts powder particles to define a part cross section. A recoating system similar to SLS machines then deposits another layer of powder, enabling the machine to print binder to define the next cross section. A wide range of polymer, metal, and ceramic materials have been processed in this manner. Several companies licensed the 3DP technology from MIT and became successful machine developers, including ZCorp and Ex One. This discussion will be continued in Sect. 7.6.

More recently, the focus of development has been on the deposition of acrylate photopolymer, wherein droplets of liquid monomer are formed and then exposed to ultraviolet light to promote polymerization. The reliance upon photopolymerization is similar to that in stereolithography, but other process challenges are significantly different. The leading edge of this second wave of machines arrived on the market with the Quadra from Objet Geometries of Israel in 2000, followed quickly by the revised QuadraTempo in 2001. Both machines jetted a photopolymer using print heads with over 1,500 nozzles [3]. In 2003, 3D Systems launched a competing technology with its InVision 3D printer. Multi-Jet Modeling, the printing system used in this machine, was actually an extension of the technology developed with the ThermoJet line [3], despite the change in material solidification strategy. The companies continue to innovate, as will be discussed in the next section.

7.1.2 Commercially Available Printing Machines

The three main companies involved in the development of the RP printing industry are still the main players offering printing-based machines: Solidscape, 3D

Systems, and Objet Geometries. Solidscape sells the T66 and T612, both descendents of the previous ModelMaker line and based upon the first-generation melted wax technique. Each of these machines employs two single jets – one to deposit a thermoplastic part material and one to deposit a waxy support material – to form layers 0.0005 in. thick [4]. It should be noted that these machines also fly-cut layers after deposition to ensure that the layer is flat for the subsequent layer. Because of the slow and accurate build style as well as the waxy materials, these machines are often used to fabricate investment castings for the jewelry and dentistry industries.

3D Systems and Objet Geometries offer machines using the ability to print and cure acrylic photopolymers. Objet Geometries markets the Eden, Alaris, and Connex series of printers. These machines print a number of different acrylic-based photopolymer materials in 0.0006 in. layers from heads containing 1,536 individual nozzles, resulting in rapid, line-wise deposition efficiency, as opposed to the slower, point-wise approach used by Solidscape. Each photopolymer layer is cured by ultraviolet light immediately as it is printed, producing fully cured models without post-curing. Support structures are built in a gel-like material, which is removed by hand and water jetting [5]. See Fig. 7.1 for an illustration of Objet's Polyjet system, which is employed in all Eden machines. The Connex500 machine is the first from Objet that provides multimaterial capability. Only two different photopolymers can be printed at one time; however, by automatically adjusting build styles, the machine can print up to 25 different effective materials by varying the relative composition of the two photopolymers.

In competition with Objet, 3D Systems markets the ProJet printers, which print layers 0.0016 inches thick using heads with hundreds of nozzles, half for part material and half for support material [6]. Layers are then flashed with ultraviolet

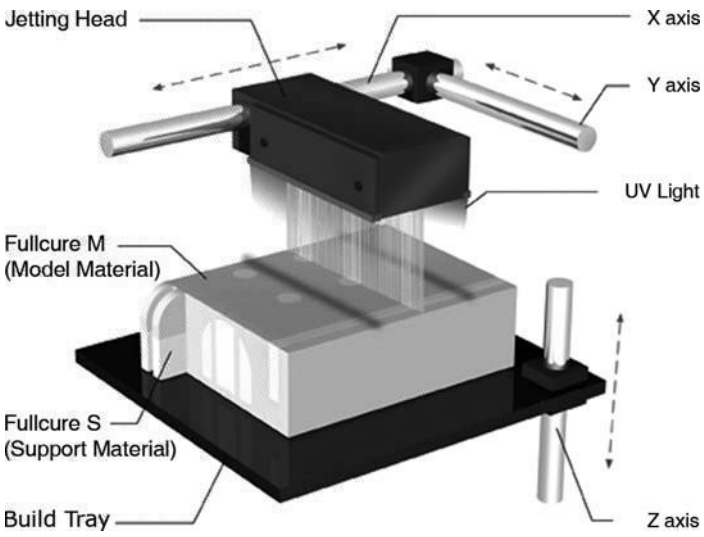

Fig. 7.1 Objet Polyjet build process [5]

light, which activates the photoinitiated polymerization. The Projets are the third generation of the Multi-Jet Modeling family from 3D Systems, following the ThermoJet described above and the InVision series. A comparison of the machines currently available is presented in Table 7.1.

7.1.3 Advantages of Printing

Each AM process has its advantages and disadvantages. The primary advantages of printing, both direct and binder printing, as an AM process include low cost, high speed, scalability, ease of building parts in multiple materials, and the capability of printing colors. Printing machines are much lower in cost than other AM machines, particularly the ones that use lasers. In general, printing machines can be assembled from standard components (drives, stages, print heads), while other machines have many more machine-specific components. High speed and scalability are related: by using print heads with hundreds or thousands of nozzles, it is possible to deposit a lot of material quickly and over a considerable area. Scalability in this context means that printing speed can be increased by adding another print head to a machine, a relatively easy task, much easier than adding another laser to a SL or SLS machine.

As mentioned, Objet markets the Connex500 machine that prints in two part materials. One can imagine adding more print heads to increase the capability to three or four materials. Compatibility and resolution need to be ensured, but it seems that these kinds of improvements should occur in the near future.

Related to multiple materials, colors can be printed by some commercial AM machines (see Sect. 7.6). The capability of printing in color is an important advance in the AM industry; for many years, parts could only be fabricated in one color. The only exception was the selectively colorable SL resins that Huntsman markets for the medical industry, which were developed in the mid-1990s. These resins were capable of only two colors, amber and either blue or red. In contrast, ZCorp markets an AM machine that prints in high resolution 24-bit color. Several companies are using these machines to produce figurines for video-gamers and other consumers (see Chaps. 3 and 11).

For completeness, a few disadvantages of printing will provide a more balanced presentation. The choice of materials to date is limited. For direct printing, only waxes and photopolymers are commercially available. For binder printing, some polymer-ceramic composites and metals are available, but they come with many limitations. Part accuracy, particularly for large parts, is generally not as good as with some other processes, notably SL and Fused Deposition Modeling. However, accuracies have been improving across the industry and are expected to improve among all processes.

Table 7.1 Commercially Available Printing-based AM Machines [4, 72–76]

Company/Product	Cost (1000s)	Build Size XxYxZ (inches)	Min. Layer (inches)	Resolution X, Y, Z (dpi)	Material	Support
Solidscape						
T66	$40	6 × 6 × 6	0.0005	25M drops	Thermoplastic	Wax
T612	$50	6 × 6 × 12	0.0005	per sq. inch		
3D Systems						
ProJect CPX 3000	–	11.7 × 7.3 × 8 (HD)	0.036mm	328,328,700	Wax	Dissolvable wax
	–	5 × 7 × 6 (XHD)	0.016mm	656,656,1600		
ProJet CP 3000	–	11.7 × 7.3 × 8	0.036mm	328,328,700		
ProJet HP 3000	–	11.7 × 7.3 × 8 (HD)	0.040mm	328,328,606		
	–	5 × 7 × 6 (UHD)	0.043mm	656,656,800		Wax; heat removal
ProJet SD 3000	–	11.7 × 7.3 × 8	0.040mm	328,328,606		
Objet						
Eden 250	$60	10.2 × 9.8 × 8.1	0.0006	600,300,1600	Acrylic photopolymer	Gel-like photopolymer; pressurized water removal
Eden 260	$80	10.2 × 9.8 × 8.1	0.0006	600,300,1600		
Eden 350(V)	$107/130	13.4 × 13.4 × 7.9	0.0006	600,600,1600		
Eden 500V	$170	19.3 × 15.4 × 7.9	0.0006	600,600,1600		
Connex500	$250	19.3 × 15.4 × 7.9	0.0006	600,600,1600		

7.2 Research Achievements in Printing Deposition

While industry players have so far introduced printing machines that use waxy polymers and acrylic photopolymers exclusively, research groups around the world have experimented with the potential for printing machines that could build in those and other materials. Among those materials most studied and most promising for future applications are polymers, ceramics, and metals. This section highlights achievements in those research areas.

7.2.1 Polymers

Polymers consist of an enormous class of materials, representing a wide range of mechanical properties and applications; only a small fraction of that range is represented by the machines discussed in Sect. 7.1. And although polymers are the only material currently used in the printing industry, there seems to be relatively little discussion on polymer inkjet production of macro three-dimensional structures in the published scientific literature.

Gao and Sonin [7] present the first notable academic study of the deposition and solidification of groups of molten polymer microdrops. They discuss findings related to three modes of deposition: columnar, sweep (linear), and repeated sweep (vertical walls). The two materials used in their investigations were a candelilla wax and a microcrystalline petroleum wax, deposited in droplets 50 μm in diameter from a print head 3–5 mm from a cooled substrate. The authors first consider the effects of droplet deposition frequency and cooling on columnar formation. As would be expected, if the drops are deposited rapidly ($\geq$50 Hz in this case), the substrate on which they impinge is still at an elevated temperature, reducing the solidification contact angle and resulting in ball-like depositions instead of columns (Fig. 7.2a). Numerical analyses of the relevant characteristic times of cooling are included. Gao and Sonin also consider horizontal deposition of droplets and the subsequent formation of lines. They propose that smooth solid lines will be formed only in a small range of droplet frequencies, dependent upon the sweep speed, droplet size, and solidification contact angle (Fig. 7.2b). Finally, they propose that wall-like deposition will involve a combination of the relevant aspects from each of the above situations.

Reis et al. [8] also provide some discussion on the linear deposition of droplets. They deposited molten Mobilwax paraffin wax with a heated print head from SolidScape. They varied both the print head horizontal speed and the velocity of droplet flight from the nozzle. For low droplet speeds, low sweep speeds created discontinuous deposition and high sweep speeds created continuous lines (Fig. 7.3a–c). High droplet impact speed led to splashing at high sweep speeds and line bulges at low sweep speeds (Fig. 7.3d–f).

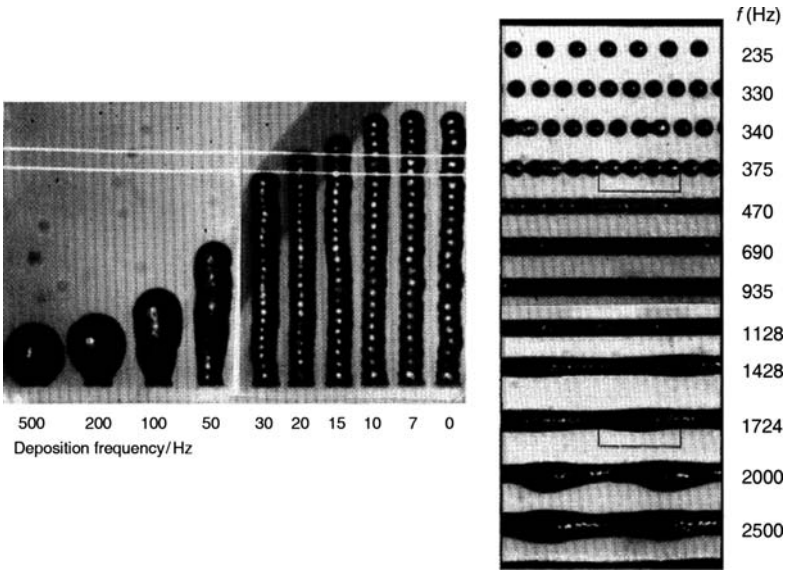

Fig. 7.2 (**a**) Columnar formation and (**b**) line formation as functions of droplet impingement frequency [7]

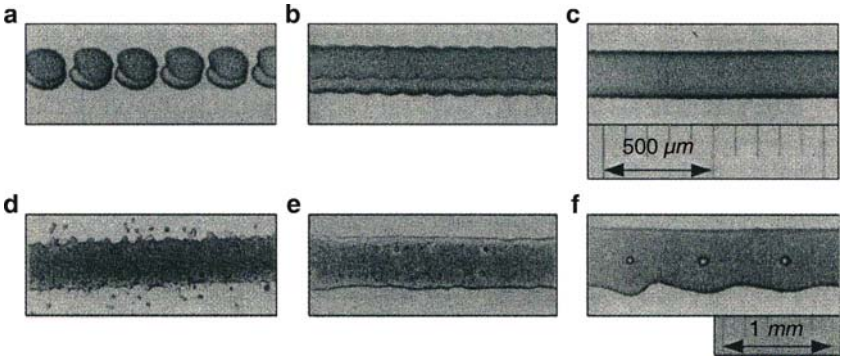

Fig. 7.3 Results of varying sweep and impact speeds [8]

From these studies, it is clear that process variables such as print head speed, droplet velocity, and droplet frequency affect the quality of the deposit. These process variables vary depending upon the characteristics of the fluid being printed, so some process development, or fine-tuning, is generally required when trying to print a new material or develop a new printing technology.

Feng et al. [9] finally present a full system, based on a print head from MicroFab Technologies Inc., that functions similarly to the commercially available machines. It prints a wax material which is heated to 80°C, more than ten degrees past its melting point, and deposits it in layers 13–60 μm thick. The deposition pattern is

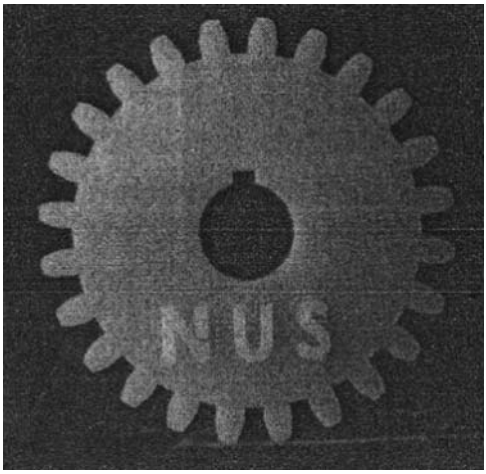

Fig. 7.4 Wax gear [9]

controlled by varying the droplet size and velocity, as well as the pitch and hatch spacing of the lines produced. An example of the result, a 2.5-dimensional gear, is presented in Fig. 7.4.

7.2.2 Ceramics

One significant advance in terms of direct printing for three-dimensional structures has been achieved in the area of ceramic suspensions. As in the case of polymers, studies have been conducted that investigate the basic effects of modifying sweep speed, drop-to-drop spacing, substrate material, line spacing, and simple multilayer forms in the deposition of ceramics [10]. These experiments were conducted with a mixture of zirconia powder, solvent, and other additives, which was printed from a 62 μm nozzle onto substrates 6.5 mm away. The authors found that on substrates that permitted substantial spreading of the deposited materials, neighboring drops would merge to form single, larger shapes, whereas on other substrates the individual dots would remain independent (see Fig. 7.5). In examples where multiple layers were printed, the resulting deposition was uneven, with ridges and valleys throughout.

A sizable body of work has been amassed in which suspensions of alumina particles are printed via a wax carrier [11]. Suspensions of up to 40% solids loading have been successfully deposited; higher concentrations of the suspended powder have resulted in prohibitively high viscosities. Because this deposition method results in a part with only partial ceramic density, the green part must be burnt out and sintered, resulting in a final product which is 80% dense but whose dimensions are subject to dramatic shrinkage [12]; a part created in this fashion is shown in Fig. 7.6.

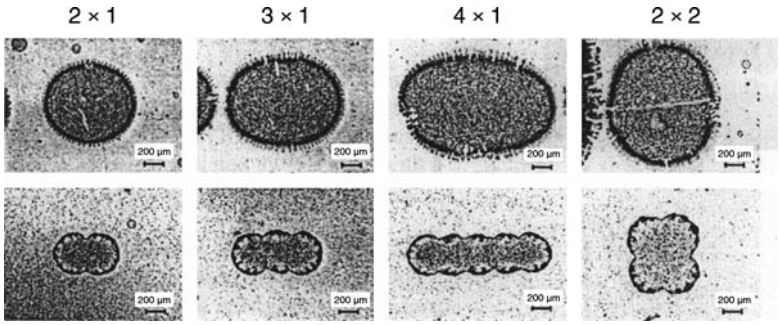

Fig. 7.5 Droplets on two different substrates [10]

Fig. 7.6 Sintered alumina impeller [12]

Similar attempts have been made with zirconia powder, using material with 14% ceramic content by volume [13], with an example shown in Fig. 7.7, as well as with PZT, up to 40% ceramic particles by volume [14].

7.2.3 Metals

Much of the printing work related to metals has focused upon the use of printing for electronics applications – formation of traces, connections, and soldering. Liu and Orme [15] present an overview of the progress made in solder droplet deposition for the electronics industry. Because solder has a low melting point, it is an obvious choice as a material for printing. Liu and Orme [15] report use of droplets of 25–500 µm, with results such as the IC test board in Fig. 7.8, which has 70 µm droplets of Sn63/Pb37. Many of the results to which they refer are those of researchers at MicroFab Technologies, who have also produced solder forms such as 25 µm diameter columns.

There is, however, some work in true three-dimensional fabrication with metals. Priest et al. [16] provide a survey of liquid metal printing technologies and history,

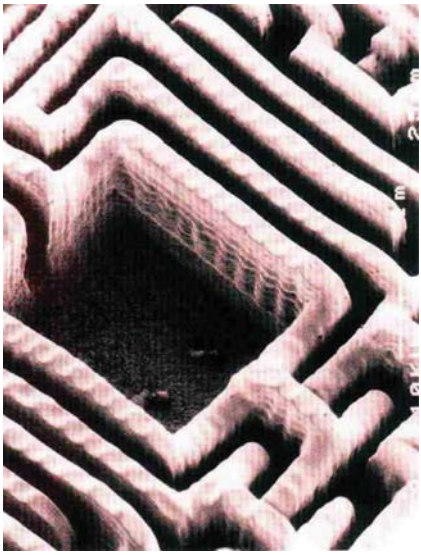

Fig. 7.7 Sintered zirconia vertical walls [13]

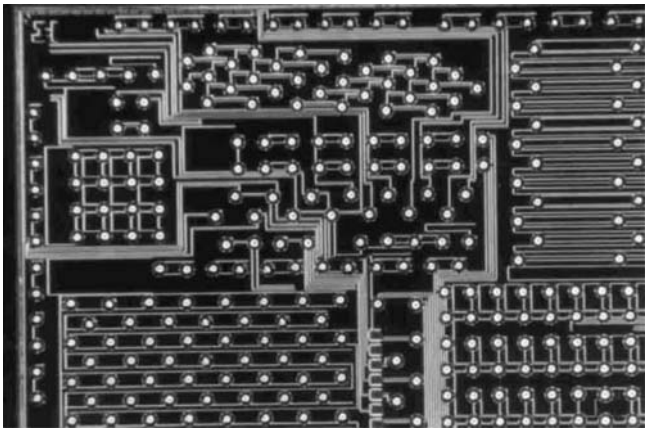

Fig. 7.8 IC test board with solder droplets [15]

including alternative technologies employed and ongoing research initiatives. Metals that had been printed included copper, aluminum, tin, various solders, and mercury. One major challenge identified for depositing metals is that the melting point of the material is often high enough to significantly damage components of the printing system.

Orme et al. [17, 18] report on a process that uses droplets of Rose's metal (an alloy of bismuth, lead, and tin). They employ nozzles of diameter 25–150 μm with resulting droplets of 47–283 μm. In specific cases, parts with porosity as low as

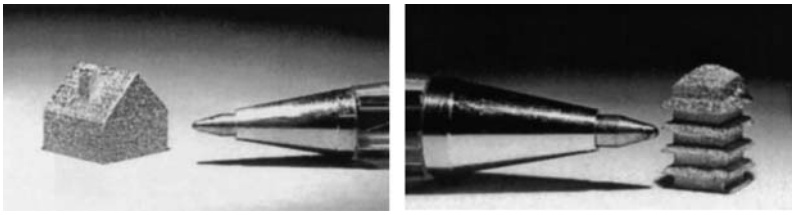

Fig. 7.9 Examples of parts fabricated with metal printing [20]

0.03% were formed without post-processing, and the microstructure formed is more uniform than that of standard casting. In discussion of this technology, considerations of jet disturbance, aerodynamic travel, and thermal effects are all presented.

Yamaguchi et al. [19, 20] used a piezoelectrically driven actuator to deposit droplets of an alloy (Bi–Pb–Sn–Cd–In), whose melting point was 47°C. They heated the material to 55°C and ejected it from nozzles 200 μm, 50 μm, and less than 8 μm in diameter. As expected, the finer droplets created parts with better resolution. The density, or "packing rate," of some parts reached 98%. Other examples of fabricated parts are shown in Fig. 7.9.

More recently, several research groups have demonstrated aluminum deposition [21, 22]. In one example, near-net shape components, with fairly simple shapes, have been formed from Al2024 alloy printed from a 100 μm orifice. In another example, pressure pulses of argon gas in the range of 20–100 KPa were used to eject droplets of molten aluminum at the rate of 1–5 drops per second. To achieve this, the aluminum was melted at 750°C and the substrate to 300°C. The nozzle orifice used was 0.3 mm in diameter, with a resulting droplet size of 200–500 μm and a deposited line of width 1.00 mm and thickness 0.17 mm. The final product was a near-net shape part of density up to 92%.

As these examples have shown, printing is well on its way to becoming a viable process for three-dimensional prototyping and manufacturing. While industry has only barely begun to use printing in this arena, the economic and efficiency advantages that printing provide ensure that it will be pursued extensively in the future. Researchers in academia have expanded the use of printing to materials such as ceramics and metals, thus providing additional prospective applications for the technology. Despite its great potential, however, the growth of printing has been hampered significantly by technical challenges inherent to the printing process. These challenges and possible solutions are investigated in subsequent sections.

7.3 Technical Challenges of Printing

As evidenced by the industry and research applications of printing discussed in the previous section, printing already has a strong foothold in terms of becoming a successful AM technology. There are, however, some serious technical shortcomings that have prevented its development from further growth. To identify and

address those problems, the relevant phenomena and strategic approaches taken by its developers must be understood. In the next two sections, the technical challenges of the printing process are outlined, the most important of its limitations relevant to the deposition of functional polymers are identified, and how those limitations are currently addressed is summarized.

Printing for three-dimensional fabrication is an extremely complex process, with challenging technical issues throughout. The first of these challenges is formulation of the liquid material. If the material is not in liquid form to begin with, this may mean suspending particles in a carrier liquid, dissolving materials in a solvent, melting a solid polymer, or mixing a formulation of monomer or prepolymer with a polymerization initiator. In many cases, other substances such as surfactants are added to the liquid to attain acceptable characteristics. Entire industries are devoted to the mixture of inks for two-dimensional printing, and it is reasonable to assume that in the future this will also be the case for three-dimensional fabrication.

The second hurdle to overcome is droplet formation. To use inkjet deposition methods, the material must be converted from a continuous volume of liquid into a number of small discrete droplets. This function is often dependent upon a finely tuned relationship between the material being printed, the hardware involved, and the process parameters; a number of methods of achieving droplet formation are discussed in Sect. 7.3.1. Small changes to the material, such as the addition of tiny particles [23], can dramatically change its droplet forming behavior as well, as can changes to the physical setup.

A third challenge is control of the deposition of these droplets; this involves issues of droplet flight path, impact, and substrate wetting or interaction [24–28]. In printing processes, either the print head or the substrate is usually moving, so the calculation of the trajectory of the droplets must take this issue into account. In addition to the location of the droplets' arrival, droplet velocity and size will also affect the deposition characteristics, as mentioned in Sect. 7.2, and must be measured and controlled via nozzle design and operation. The quality of the impacted droplet must also be controlled: if smaller droplets, called satellites, break off from the main droplet during flight, then the deposited material will be spread over a larger area than intended and the deposition will not have well-defined boundaries. In the same way, if the droplet splashes on impact, forming what is called a "crown," similar results will occur [29]. All of the effects will negatively impact the print quality of the printed material.

Concurrently, the conversion of the liquid material droplets to solid geometry must be carefully controlled; as discussed in Sect. 7.2, direct printing relies on a phase change of the printed material. Examples of phase change modes employed in existing printing technologies are: solidification of a melted material (e.g., wax, solder), evaporation of the liquid portion of a solution (e.g., some ceramic approaches), and curing of a photopolymer (e.g., Objet, ProJet machines) or other chemical reactions. The phase change must occur either during droplet flight or soon after impact; the time and place of this conversion will also affect the droplet's interaction with the substrate [30, 31] and the final deposition created. To further

complicate the matter, drops may solidify nonuniformly, creating warpage and other undesirable results [32].

In direct printing, an additional challenge arises: that of controlling deposition atop layers of previous deposition rather than only upon the initial substrate [7, 10]. The droplets will interact differently, for example, with a metal plate substrate than with a surface of previously printed wax droplets. To create substantive three-dimensional parts, each layer deposited must be fully bound to the previous layer to prevent delamination, but must not damage that layer while being created. Commercially available machines tend to approach this problem by employing devices that plane or otherwise smooth the surface periodically [32–34].

Operational considerations also pose a challenge in process planning for printing. For example, because nozzles are so small, they often clog, preventing droplets from exiting. Much attention has been given to monitoring and maintaining nozzle performance during operation [32]. Most machines currently in use go through purge and cleaning cycles during their builds to keep as many nozzles open as possible; they may also wipe the nozzles periodically [33]. Some machines may also employ complex sensing systems to identify and compensate for malfunctioning or inconsistent nozzles [35, 36]. In addition, many machines, including all commercial AM machines, have replaceable nozzles in case of permanent blockage.

Finally, to achieve the best print resolution, it is advantageous to produce many small droplets very close together. However, this requires high nozzle density in the print head, which is unattainable for many nozzle manufacturing processes. An alternative to nozzle density is to make multiple passes over the same area, effectively using process planning instead of hardware to create the desired effect [33]. Even in cases where high nozzle density is possible, however, problems arise due to crosstalk – basically an "overlapping" of the thermal or pressure differentials used to drive adjacent nozzles.

In approaching a printing process, these numerous challenges must in some sense be addressed sequentially: flight pattern cannot be studied until droplets are formed and layering cannot be investigated until deposition of single droplets is controlled. In terms of functional polymer deposition, the challenge of material preparation has effectively been addressed; numerous polymer resins and mixtures already exist. It is the second challenge – droplet formation – that is therefore the current limiting factor in deposition of these materials. To understand these limitations, Sect. 7.3.1 reviews the dynamic processes that are currently used to form droplets and Sect. 7.5 considers necessary methods of modifying the printing material for use with those processes.

7.3.1 Droplet Formation Technologies

Over the time that two-dimensional inkjet printing has evolved, a number of methods for creating and expelling droplets has been developed. The main

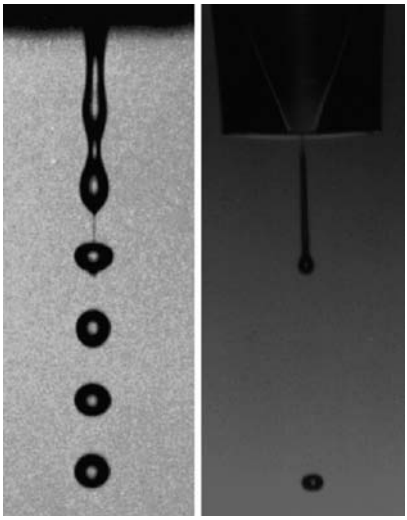

Fig. 7.10 Continuous (*left*) and drop-on-demand (*right*) deposition [39]

distinction in categorizing the most common of technologies refers to the possible modes of expulsion: continuous stream (CS) and drop-on-demand (DOD). This distinction refers to the form in which the liquid exits the nozzle – as either a continuous column of liquid or as discrete droplets. Figure 7.10 shows the distinction between continuous (left) and DOD (right) formations.

7.3.2 Continuous Mode

In CS mode, a steady pressure is applied to the fluid reservoir, causing a pressurized column of fluid to be ejected from the nozzle. After departing the nozzle, this stream breaks into droplets due to Rayleigh instability. The breakup can be made more consistent by vibrating, perturbing, or modulating the jet at a fixed frequency close to the spontaneous droplet formation rate, in which case the droplet formation process is synchronized with the forced vibration, and ink droplets of uniform mass are ejected [37]. Because droplets are produced at constant intervals, their deposition must be controlled after they separate from the jet. To achieve this, they are introduced to a charging field and thus attain an electrostatic charge. These charged particles then pass through a deflection field, which directs the particles to their desired destinations – either a location on the substrate or a container of material to be recycled or disposed. Figure 7.11 shows a schematic of the function of this type of binary deflection continuous system.

An advantage of CS deposition is the high throughput rate; it has therefore seen widespread use in applications such as food and pharmaceutical labeling [38]. Two major constraints related to this method of droplet formation are, however, that the

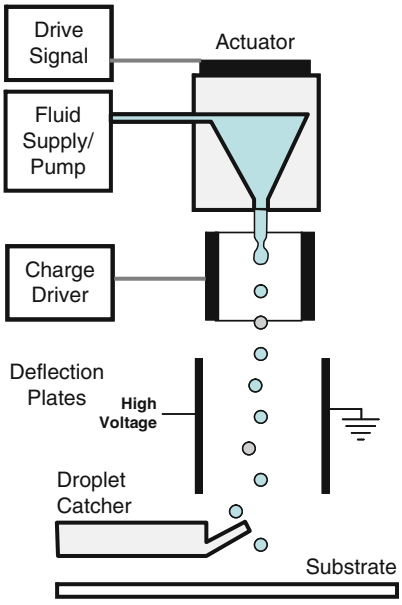

Fig. 7.11 Binary deflection continuous printing [39]

materials must be able to carry a charge and that the fluid deflected into the catcher must be either disposed of or reprocessed, causing problems in cases where the fluid is costly or where waste management is an issue.

In terms of droplets formed, commercially available systems typically generate droplets that are about 150 µm in diameter at a rate of 80–100 kHz, but frequencies of up to 1 MHz and droplet sizes ranging from 6 µm (10 fl) to 1 mm (0.5 µl) have been reported [39]. It has also been shown that, in general, droplets formed from continuous jets are almost twice the diameter of the undisturbed jet [40].

A few investigators of three-dimensional deposition have opted to use continuous printing methods. Blazdell et al. [41] used a continuous printer from Biodot, which was modulated at 66 kHz while ejecting ceramic ink from 50 and 75 µm nozzles. They used 280 kPa of air pressure. Blazdell [42] reports later results in which this Biodot system was modulated at 64 kHz, using a 60 µm nozzle that was also 60 µm in length. For much of the development of the 3DP process, CS deposition was used. At present, the commercial machines based on 3DP (from ZCorp and Ex One) use standard DOD print heads. A representative ceramic ink used with this system was a suspension of ultra-fine particles 2.4% solid loading by volume, with a resultant viscosity of 1.11 cP and a surface tension of 24.5 mN/m [40]. In metal fabrication, Tseng et al. [43] used a continuous jet in depositing their solder alloy, which had a viscosity of about 2 cP at the printing temperature. Orme et al. [17, 18] also report the use of an unspecified continuous system in deposition of solders and metals.

7.3.3 *Drop-on-Demand Mode*

In DOD mode, in contrast, individual droplets are produced directly from the nozzle. Droplets are formed only when individual pressure pulses in the nozzle cause the fluid to be expelled; these pressure pulses are created at specific times by thermal, electrostatic, piezoelectric, acoustic, or other actuators [1]. Figure 7.12 shows the basic functions of a DOD setup. Liu and Orme [15] assert that DOD methods can deposit droplets of 25–120 µm at a rate of 0–2000 drops per second.

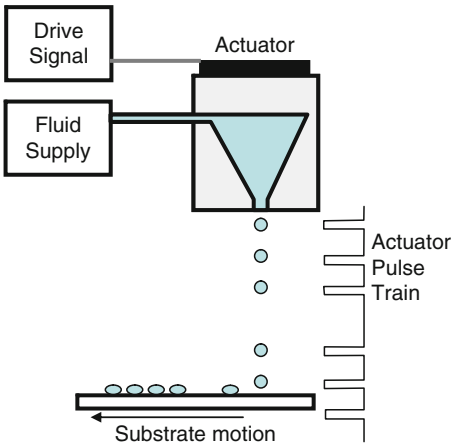

Fig. 7.12 Schematic of drop-on-demand printing system [39]

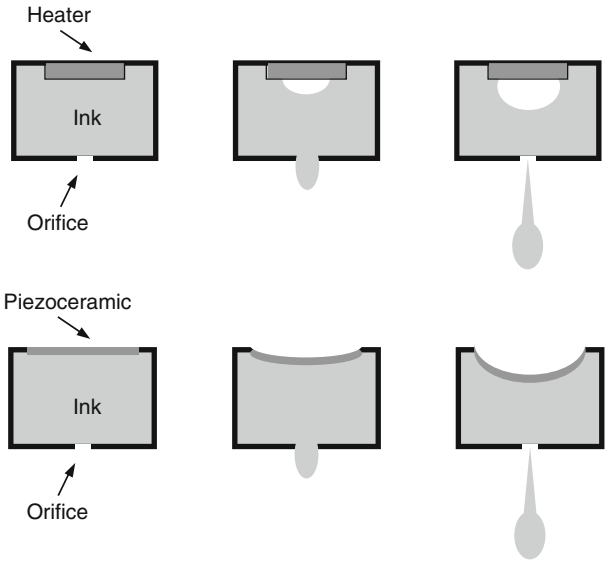

Fig. 7.13 Thermal (*top*) and piezoelectric (*bottom*) DOD ejection

In the current DOD printing industry, thermal (bubble-jet) and piezoelectric actuator technologies dominate; these are shown in Fig. 7.13. Thermal actuators rely on a resistor to heat the liquid within a reservoir until a bubble expands in it, forcing a droplet out of the nozzle. Piezoelectric actuators rely upon the deformation of a piezoelectric element to reduce the volume of the liquid reservoir, which causes a droplet to be ejected. As noted by Basaran [44], the waveforms employed in piezoelectrically driven DOD systems can vary from simple positive square waves to complex negative–positive–negative waves in which the amplitude, duration, and other parameters are carefully modulated to create the droplets as desired.

In their review of polymer deposition, De Gans et al. [38] assert that DOD is the preferable method for all applications that they discuss due to its smaller drop size (often of diameter similar to the orifice) and higher placement accuracy in comparison to CS methods. They further argue that piezoelectric DOD is more widely applicable than thermal because it does not rely on the formation of a vapor bubble or on heating that can damage sensitive materials.

The preference for piezoelectrically driven DOD printing is reflected in the number of investigators who use and study such setups. For example, Gao and Sonin [7] use this technology to deposit 50 µm droplets of two waxes, whose viscosity at 100°C is about 16 cP. Sirringhaus et al. [45] and Shimoda et al. [46] both use piezoelectric DOD deposition for polymer solutions, as discussed in Sect. 7.5.2. In ceramic deposition, Reis et al. [8] print mixtures with viscosities 6.5 and 14.5 cP at 100°C and frequencies of 6–20 kHz. Yamaguchi et al. [19, 20] also used a piezoelectrically driven DOD device at frequencies up to 20 Hz in the deposition of metal droplets. Similarly, the solder droplets on the circuit board in Fig. 7.8 were also deposited with a DOD system.

At present, all commercial AM printing machines use DOD print heads, generally from a major manufacturer of printers or printing technologies. Such companies include Hewlett-Packard, Canon, Dimatix, and Xaar.

7.3.4 Other Droplet Formation Methods

Aside from the standard CS and DOD methods, other technologies have been experimentally investigated but have not enjoyed widespread use in industry applications. Liquid spark jetting, a relative of thermal printing, relies on an electrical spark discharge instead of a resistor to form a gas bubble in the reservoir [47]. The electrohydrodynamic inkjet employs an extremely powerful electric field to pull a meniscus and, under very specific conditions, droplets from a pressure-controlled capillary tube [47]; these droplets are significantly smaller than the tube from which they emanate. Electro-rheological fluid jetting uses an ink whose properties change under high electric fields; the fluid flows only when the electric field is turned off [47]. In their flextensional ultrasound droplet ejectors, Percin and Khuri-Yakub [48] demonstrate both DOD and continuous droplet formation with a

system in which a plate containing the nozzle orifice acts as the actuator, vibrating at resonant frequencies and forming droplets by creating capillary waves on the liquid surface as well as an increased pressure in the liquid. Focused acoustic beam ejection uses a lens to focus an ultrasound beam onto the free surface of a fluid, using the acoustic pressure transient generated by the focused tone burst to eject a fluid droplet [49]. Meacham et al. extended this work [50] to develop an inexpensive ultrasonic droplet generator and developed a fundamental understanding of its droplet formation mechanisms [51]. These ultrasonic droplet generators show promise in ejecting viscous polymers [52]. Fukumoto et al. [53] present a variant technology in which ultrasonic waves are focused onto the surface of the liquid, forming surface waves that eventually break off into a mist of small droplets. Overviews of these various droplet formation methods are given by Lee [47] and Basaran [44].

7.4 Printing Process Modeling

Conservation of energy concepts provides an appropriate context for investigating droplet generation mechanisms for printing. Essentially, the energy imparted by the actuation method to the liquid must be sufficient to balance three requirements: fluid flow losses, surface energy, and kinetic energy. The losses originate from a conversion of kinetic energy to thermal energy due to the viscosity of the fluid within the nozzle; this conversion can be thought of as a result of internal friction of the liquid. The surface energy requirement is the additional energy needed to form the free surface of the droplet or jet. Finally, the resulting droplet or jet must still retain enough kinetic energy to propel the liquid from the nozzle toward the substrate. This energy conservation can be summarized as

$$E_{\text{imparted}} = E_{\text{loss}} + E_{\text{surface}} + E_{\text{kinetic}} \tag{7.1}$$

The conservation law can be considered in the form of actual energy calculations or in the form of pressure, or energy per unit volume, calculations. For example, Sweet used the following approximation for the gauge pressure required in the reservoir of a continuous jetting system [54]:

$$\Delta p = 32\mu d_{\text{j}}^2 v_{\text{j}} \int_{l_1}^{l_2} \frac{dl}{d_n^4} + \frac{2\sigma}{d_{\text{j}}} + \frac{\rho v_{\text{j}}^2}{2} \tag{7.2}$$

where, Δp is the total gauge pressure required, μ is the dynamic viscosity of the liquid, ρ is the liquid's density, σ is the liquid's surface tension, d_{j} is the diameter of the resultant jet, d_n is the inner diameter of the nozzle or supply tubing, v_{j} is the velocity of the resultant jet, and l is the length of the nozzle or supply tubing. The

first term on the right of (7.2) is an approximation of the pressure loss due to viscous friction within the nozzle and supply tubing. The second term is the internal pressure of the jet due to surface tension; the third term is the pressure required to provide the kinetic energy of the droplet or jet.

Energy conservation can also be thought of as a balance among the effects before the fluid crosses a boundary at the orifice of the nozzle and after it crosses that boundary. Before the fluid leaves the nozzle, the positive effect of the driving pressure gradient accelerates it, but energy losses due to viscous flow decelerate it. The kinetic energy with which it leaves the nozzle must be enough to cover the kinetic energy of the traveling fluid as well as the surface energy of the new free surface.

As indicated earlier, actuation energy is typically in the form of heating (bubble-jet) or vibration of a piezoelectric actuator. Various electrical energy waveforms may be used for actuation. In any event, these are standard types of inputs and will not be discussed further.

While the liquid to be ejected travels through the nozzle, before forming droplets, its motion is governed by the standard equations for incompressible, Newtonian fluids, as we are assuming these flows to be. The flow is fully described by the Navier–Stokes and continuity equations; however, these equations are difficult to solve analytically, so we will proceed with a simplification. The first term on the right side of (7.2) takes advantage of one situation for which an analytical solution is possible, that of steady, incompressible, laminar flow through a straight circular tube of constant cross section. The solution is the Hagen–Poiseuille law [55], which reflects the viscous losses due to wall effects:

$$\Delta p = \frac{8Q\mu l}{\pi r^4 \sigma} \tag{7.3}$$

where Q is the flow rate and r is the tube radius. Note that this expression is most applicable when the nozzle is a long, narrow glass tube. However, it can also apply when the fluid is viscous, as we will see shortly.

Another assumption made by using the Hagen–Poiseuille equation is that the flow within the nozzle is fully developed. For the case of laminar flow in a cylindrical pipe, the length of the entry region l_e where flow is not yet fully developed is defined as 0.06 times the diameter of the pipe, multiplied by the Reynolds number [55]:

$$l_e = 0.06d\mathrm{Re} = \frac{0.06\rho\bar{v}d^2}{\mu} \tag{7.4}$$

where $\bar{v}$ is the average flow velocity across the pipe. To appreciate the magnitude of this effect, consider printing with a 20 μm nozzle in a plate that is 0.1 mm thick, where the droplet ejection speed is 10 m/s. The entry lengths for a fluid with the density of water and varying viscosities are shown in Table 7.2.

Table 7.2 Entry lengths for "water" at various viscosities

Viscosity (cP)	Density (kg/m^3)	Entry length (μm)
1	1,000	240
	1,250	300
10	1,000	24
	1,250	30
40	1,000	6
	1,250	7.5
100	1,000	2.4
	1,250	3
200	1,000	1.2
	1,250	1.5

Entry lengths are a small fraction of the nozzle length for fluids with viscosities of 40 cP or greater. As a result, we can conclude that flows are fully developed through most of a nozzle for fluids that are at the higher end of the range of printable viscosities.

Most readers will have encountered the primary concepts of fluid mechanics in an undergraduate course and may be familiar with the Navier–Stokes equation, viscosity, surface tension, etc. As a reminder, viscosity is a measure of the resistance of a fluid to being deformed by shear or extensional forces. We will restrict our attention to dynamic, or absolute, viscosity, which has units of pressure-time; in the SI system, units are typically Pa·s or mPa·s, for milli-Pascals·seconds. Viscosity is also given in units of poise or centipoises, named after Jean Louis Marie Poiseuille. Centipoise is abbreviated cP, which conveniently has the same magnitude as mPa·s. That is, 1 cP is equal to 1 mPa s. Surface tension is given in units of force per length, or energy per unit area; in the SI system, surface tension often has units of N/m or J/m^2.

We can investigate the printing situation further by computing the pressures required for ejection. Equation (7.3) will be used to compute the pressure required to print droplets for various fluid viscosities and nozzle diameters. For many printing situations, wall friction dominates the forces required to print, hence we will only investigate the first term on the right of (7.2) and ignore the second and third terms (which are at least one order of magnitude smaller than wall friction).

Figure 7.14 shows how the pressure required to overcome wall friction varies with fluid viscosity and nozzle diameter. As can be seen, pressure needs increase sharply as nozzles vary from 0.1 to 0.02 mm in diameter. This could be expected, given the quadratic dependence of pressure on diameter in (7.3). Pressure is seen to increase linearly with viscosity, which again can be expected from (7.3). As indicated, wall friction dominates for many printing condition. However, as nozzle size increases, the surface tension of the fluid becomes more important. Also, as viscosity increases, viscous losses become important, as viscous fluids can absorb considerable acoustic energy. Regardless, this analysis provides good insight into pressure variations under many typical printing conditions.

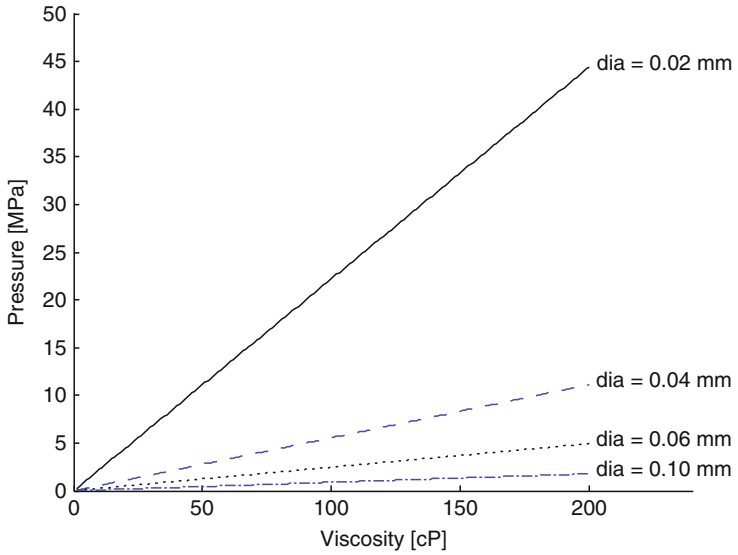

Fig. 7.14 Pressure required to overcome wall friction for printing through nozzles of different diameters

Fluid flows when printing are almost always laminar; i.e., the Reynolds number is less than 2,100. As a reminder, the Reynolds number is

$$\mathrm{Re} = \frac{\rho v r}{\mu} \tag{7.5}$$

Another dimensionless number of relevance in printing is the Weber number, which describes the relative importance of a fluid's inertia compared with its surface tension. The expression for the Weber number is:

$$\mathrm{We} = \frac{\rho v^2 r}{\gamma} \tag{7.6}$$

Several research groups have determined that a combination of the Reynolds and Weber numbers is a particularly good indication of the potential for successful printing of a fluid [12]. Specifically, if the ratio of the Reynolds number to the square root of the Weber number has a value between 1 and 10, then it is likely that ejection of the fluid will be successful. This condition will be called the "printing indicator" and is

$$1 \leq \frac{\mathrm{Re}}{\mathrm{We}^{1/2}} = \frac{\sqrt{\rho r \gamma}}{\mu} \leq 10 \tag{7.7}$$

Table 7.3 Reynolds numbers and printing indicator values for some printing conditions

Nozzle diameter [mm]	Viscosity [cP]	Reynolds no.	Printing indicator
0.02	1	20	26.8
	10	2	2.68
	40	0.5	0.67
	100	0.2	0.27
0.05	1	50	42.4
	10	5	4.24
	40	1.25	1.06
	100	0.5	0.42
0.1	1	100	60
	10	10	6
	40	2.5	1.5
	100	1	0.6

The inverse of the printing indicator is another dimensionless number called the Ohnsorge number, that relates viscous and surface tension forces. Note that values of this ratio that are low indicate that flows are viscosity limited, while large values indicate flows that are dominated by surface tension. The low value of 1 for the printing indicator means that the maximum fluid viscosity should be between 20 and 40 cP.

Some examples of Reynolds numbers and printing indicators are given in Table 7.3. For these results, the surface tension is 0.072 N/m and the density is 1,000 kg/m^3 (same as water at room temperature).

It is important to realize that the printing indicator is a guide, not a law to be followed. Water is usually easy to print through most print-heads, regardless of the nozzle size. But the printing indicator predicts that water (with a viscosity of 1 cP) should not be ejectable since its surface tension is too high. We will see in the next section how materials can be modified to make printing feasible.

7.5 Material Modification Methods

For the droplet formation methods discussed above, the maximum printable viscosity threshold is reported by a number of sources to be in the range of 20–40 cP at the printing temperature [11, 38, 56], although De Gans et al. [57] contend that they have used a micropipette optimized for polymer printing applications that was able to print Newtonian fluids with viscosities up to 160 cP. While other factors such as liquid density or surface tension and print head or nozzle design may affect the results, this limitation on viscosity quickly becomes the most problematic aspect for droplet formation of functional polymers and most other materials desirable for use in three-dimensional printing settings.

The current method of addressing this issue is to lower the viscosity of the material to be printed. The most common practices of using heat, solvents, or lower viscosity components are explored in the following sections. In addition to these

methods, it is also possible that in some polymer deposition cases shear thinning might occur, dependent upon the material or solution in use; DOD printers are expected to produce strain rates of 10^3–10^4, which should be high enough to produce shear-thinning effects [11, 58].

7.5.1 Hot Melt Deposition

The earliest and most often used solution to the problem of high viscosity is to heat the material until its viscosity drops to an acceptable point. As discussed in Sect. 7.2, for example, commercial machines such as 3D Systems' ThermoJet and Solidscape's T66 all print proprietary thermoplastics, which contain mixtures of various waxes and polymers that are solid at ambient temperatures but convert to a liquid phase at elevated printing temperatures [6]. In developing their hot melt materials, for example, 3D Systems investigated various mixtures consisting of a low shrinkage polymer resin, a low viscosity material such as paraffin wax, a microcrystalline wax, a toughening polymer, and a small amount of plasticizer, with the possible additions of antioxidants, coloring agents, or heat dissipating filler [59]. These materials were formulated to have a viscosity of 18–25 cP and a surface tension of 24–29 dynes/cm at the printing temperature of 130°C.

Much of the deposition of metals and ceramics, as well, is based upon this hot melt practice. Derby and Reis [11], for example, rely upon a melted wax as the carrier for their ceramic particles. The viscosities of these materials ranged from 2.9 to 38.0 cP at a measurement temperature of 100°C. This is also the approach taken by all of the solder and metal deposition processes; they simply heat the metal past its melting point and until the viscosity drops sufficiently. Orme et al. [60], for example, use a solder whose viscosity is approximately 1.3 cP, continuously printed under a pressure of 138 kPa.

7.5.2 Solution- and Dispersion-Based Deposition

As hot-melt deposition has very specific requirements for the material properties of what is printed, many current applications have turned to solution- or dispersion-based deposition. This allows the delivery of solids or high-molecular weight polymers in a carrier liquid of viscosity low enough to be successfully printed. De Gans et al. [38] provided a review of a number of polymeric applications in which this strategy is employed.

A number of investigators have used solution and dispersion techniques in accurate deposition of very small amounts of polymer in thin layers for meso-scale applications, such as polymer light-emitting displays, electronic components, and surface coatings and masks. For example, Shimoda et al. [46] present a technique to develop light-emitting polymer diode displays using inkjet deposition

of conductive polymers. Three different electroluminescent polymers (polyfluorine and two derivatives) were printed in organic solvents at 1–2 wt%. As another example, De Gans et al. [38] report a number of other results related to the creation of polymer light-emitting displays: a precursor of poly(*p*-phenylene vinylene) (PPV) was printed as a 0.3%wt solution; and PPV derivatives were printed in 0.5–2.0 wt% solutions in solvents such as tetraline, anisole, and o-xylene. Such low weight percentages are typical.

In deposition of ceramics, the use of a low-viscosity carrier is also a popular approach. Tay and Edirisinghe [10], for example, used ceramic powder dispersed in industrial methylated spirit with dispersant, binder, and plasticizer additives resulting in a material that was 4.5% zirconia by volume. The resulting material had a viscosity of 3.0 cP at 20°C and a shear rate of 1,000 s^{-1}. Zhao et al. [61] tested various combinations of zirconia and wax carried in octane and isopropyl alcohol, with a dispersant added to reduce sedimentation. The viscosities of these materials were 0.6–2.9 cP at 25°C; the one finally selected was 14.2% zirconia by volume.

Despite the success of solution and dispersion deposition for these specific applications, however, there are some serious drawbacks, especially in considering the potential for building more macro structures. The low concentrations of polymer and solid used in the solutions and dispersions will restrict the total amount of material that can be deposited. Additionally, it can be difficult to control the deposition pattern of this material within the area of the droplet's impact. Shimoda et al. [46], among others, report the formation of rings of deposited material around the edge of the droplet. They attribute this to the fact that the contact line of the drying drop is pinned on the substrate. As the liquid evaporates from the edges, it is replenished from the interior, carrying the solutes to the edge. They contend that this effect can be mitigated by control of the droplet drying conditions. Tay and Edirisinghe [10] report a very similar result in terms of zirconia migration during their deposition of ceramic ink droplets and give similar explanations as to the cause.

Another difficulty with solutions or dispersions, especially those based on volatile solvents, is that use of these materials can result in precipitations forming in the nozzle after a very short period of time [57], which can clog the nozzle, making deposition unreliable or impossible.

7.5.3 Prepolymer Deposition

The most recent development in addressing the issues of viscosity is the use of prepolymers in the fabrication of polymer parts. This is the method currently employed by the two newest commercially available machine lines, as discussed in Sect. 7.1.2. For example, 3D Systems investigated a series of UV-curable printing materials, consisting of mixtures of high molecular weight monomers and oligomers such as urethane acrylate or methacrylate resins, urethane waxes, low molecular weight monomers and oligomers such as acrylates or methacrylates

that function as diluents, a small amount of photoinitiators, and other additives such as stabilizers, surfactants, pigments, or fillers [62, 63]. These materials also benefited from the effects of hot melt deposition, as they were printed at a temperature of 70–95°C, with melting points between 45 and 65°C. At the printing temperatures, these materials had a viscosity of about 10–16 cP.

One problem encountered, and the reason that the printing temperatures cannot be as high as those used in hot melt deposition, is that when kept in the heated state for extended periods of time, the prepolymers begin to polymerize, raising the viscosity and possibly clogging the nozzles when they are finally printed [63]. Another complication is that the polymerization reaction, which occurs after printing, must be carefully controlled to assure dimensional accuracy.

Summary: While the general challenges of direct printing for three-dimensional fabrication are identified, there are many aspects that are not well or fully understood. Open research questions abound in almost all stages of the printing process – droplet formation, deposition control, and multilayer accumulation. For the case of functional polymer printing, the most appropriate limitation to address is that of droplet formation. Because systems developed for inviscid materials are being used for these applications, numerous accommodations and limitations currently exist; users commonly handle this by modifying the materials to fit the requirements of the existing hardware. However, if the method of droplet formulation could be modified instead, this might allow the deposition of a wider range of materials. A recently developed acoustic focusing ultrasonic droplet generator, under investigation at Georgia Institute of Technology, employs a strategy different from those of existing technologies, which may provide the capabilities to fulfill this need.

7.6 Three-Dimensional Printing

7.6.1 Technology

Three-Dimensional Printing (3DP) was invented at MIT and has been licensed to more than five companies for commercialization. In contrast to the printing processes described earlier in the chapter, 3DP prints a binder into a powder bed to fabricate a part. Hence, in 3DP, only a small portion of the part material is delivered through the print-head; most of the part material is comprised of powder in the powder bed. Typically, binder droplets (80 μm in diameter) form spherical agglomerates of binder liquid and powder particles as well as provide bonding to the previously printed layer. Once a layer is printed, the powder bed is lowered and a new layer of powder is spread onto it (typically via a counter-rotating rolling mechanism) [64], very similar to the recoating methods used in powder bed fusion processes, as presented in Chap. 5. This process (printing binder into bed; recoating bed with new layer of powder) is repeated until the part, or array of parts, is completed. A schematic of the 3DP process is shown in Fig. 7.15.

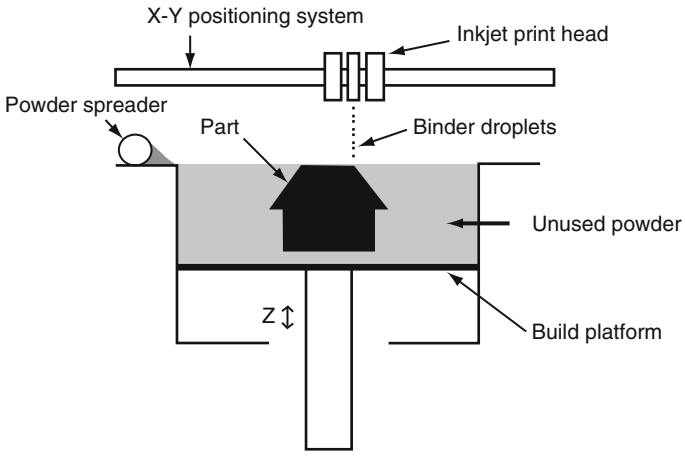

Fig. 7.15 Schematic of the 3DP process

Because the printer head contains several ejection nozzles, 3DP features several parallel one-dimensional avenues for patterning. Since the process can be economically scaled by simply increasing the number of printer nozzles, the process is considered a line-wise patterning process. Such embodiments typically have a high deposition speed at a relatively low cost (due to the lack of a high-powered energy source) [64], which is the case for 3DP machines.

The printed part is typically left in the powder bed after its completion in order for the binder to fully set and for the green part to gain strength. Post-processing involves removing the part from the powder bed, removing unbound powder via pressurized air, and infiltrating the part with an infiltrant to make it stronger and possibly to impart other mechanical properties.

The 3DP process shares many of the same advantages of powder bed processes. Parts are self-supporting in the powder bed so that support structures are not needed. Similarly to other processes, parts can be arrayed in one layer and stacked in the powder bed to greatly increase the number of parts that can be built at one time. Finally, assemblies of parts and kinematic joints can be fabricated since loose powder can be removed between the parts.

7.6.2 Commercial Machines

A wide variety of powder and binder materials can be used which enables significant flexibility in the process. MIT licensed the 3DP technology according to the type of material and application that each licensee was allowed to exploit. Z-Corporation, Inc. is one company that markets machines that build concept models in starch and plaster powder using a low viscosity glue as binder. Other materials are also

Table 7.4 Machine specifications for 3DP binder printing machines

Company/ models	Cost ($)	Deposition rate (layer/min)	Build size ($l \times w \times h$) (mm)	Resolution (DPI)	Layer thickness (mm)	Number of nozzles	Materials
ZCorp. ZPrinter 310 Plus	19,900	2–4	$200 \times 250 \times 200$	300×450	0.09–0.20	304	Composite, elastomer, direct casting, investment casting
ZPrinter 450	30,000	2–4	$200 \times 250 \times 200$	300×450	0.09–0.10	604	Composite
Spectrum Z510	50,000	2–4	$250 \times 356 \times 200$	600×540	0.089–0.20	1216	Composite, elastomer, direct casting
Ex One/R1	85,000						316 SS + Bronze, 420 SS + Bronze
Ex One/R2	125,000						316 SS + Bronze, 420 SS + Bronze
S15	1,200,000	20 mm/h	$1500 \times 750 \times 700$				Casting sand

available. At the other end of the spectrum, ExOne markets machines that build in metal powder, with a strong polymer material that is used as the binder.

As of January 2008, ZCorp. markets three models of printers, the ZPrinter 310 Plus, the ZPrinter 450, and the Spectrum Z510. The unique feature of the 450 and Z510 models is the capability of printing in color. One set of printing nozzles deposits binder, while the remaining nozzles print color. ZCorp. claims that the Z510 printer can print in 24-bit color.

Some specifications of these machines are shown in Table 7.4.

The Ex One Corporation markets a line of 3DP machines that fabricate metal parts and sand casting molds and cores in foundry sand. Strong polymer binders are required with these heavy powders. Fully dense parts can be fabricated by printing binder into the metal bed, burning off the binder in a furnace at a low temperature, sintering the metal powder during a high temperature furnace cycle, then infiltrating a second metal, such as copper or bronze, at a low temperature. The printed part, when removed from the bed, is a relatively low-density (50%) green part. Other than how the green part is formed, this process is identical to the indirect processing approach for metal and ceramic part fabrication discussed in Chap. 5 and illustrated in Fig. 5.7. Stainless steel-bronze parts have been made with this technology [65]. The process is typically accurate to ± 0.125 mm. Several ExOne machine models are also listed in Table 7.4.

Applications for the R1 and R2 models include prototypes of metal parts and some low-volume manufacturing, as well as tooling. As parts are fabricated in a powder bed, the surface finish of these parts is comparable to PBF parts, such as made by SLS. Finish machining is thus required for high tolerance and mating surfaces. ExOne markets another machine that fabricates gold dental restorations, for example copings for crowns. The materials and binder printing system were developed specifically for this application, since higher resolution is needed.

In the tooling area, Ex One promotes the advantages of conformal cooling in injection molds. In conformal cooling, cooling channels are routed close to the surfaces of the part cavity, particularly where hot spots are predicted. Using conventional machining processes, cooling channels are drilled as straight holes. With AM processes, however, cooling channels of virtually any shape and configuration can be designed into tools. Figure 7.16 illustrates one tool design with conformal cooling channels that was fabricated in an Ex One machine [65].

The largest machine, the S15, is intended for companies with large demands for castings, such as the automotive, truck, and heavy equipment industries. As of 2007, at least 19 of these machines have been installed. The machines print molds and cores for sand casting. Various metals can be cast into the printed molds, including aluminum, zinc, and even magnesium. Special equipment was developed for handling the large volumes of powders and heavy vats, including a silo and powder conveyor, conveyor track for transporting vats of powder and finished molds, and a debinding station. A typical installation with a S15 machine occupies a room 40–50 m^2 in size.

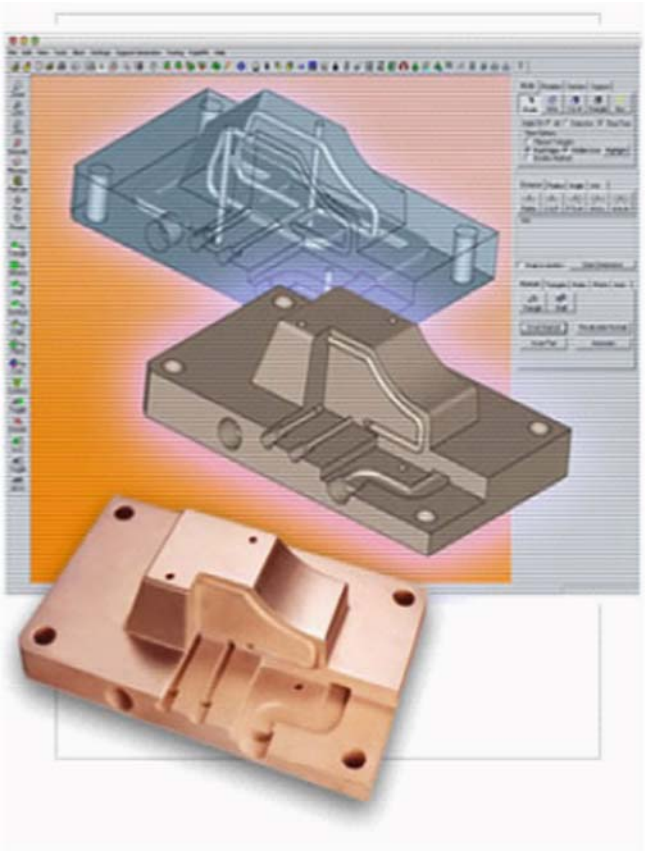

Fig. 7.16 Injection mold with conformal cooling channels fabricated in an Ex One machine (Courtesy ProMetal LLC, an Ex One Company)

7.6.3 Other Materials

A wide range of materials has been developed for 3DP, mostly by researchers. Printing into a metal powder bed was first demonstrated in the early 1990s. Concurrently, investigations into ceramic materials were also pursued.

Traditional powder-based 3DP of ceramics involves the selective printing of a binder over a bed of ceramic powder [66]. Fabrication of ceramic parts follows a very similar process compared with metal parts. Green parts created by this process are subjected to a thermal decomposition prior to sintering to remove the polymer binder. After binder burn-off, the furnace temperature is increased until the ceramic's sintering temperature is reached. Sometimes an infiltrant is used that reacts to form a ceramic binder. Another possibility is to infiltrate with a metal to form a ceramic-metal composite. The first report of using 3DP for the fabrication of ceramics was in

1993; fired components were reported as typically greater than 99.2% dense [66]. Alumina, silica, and titanium dioxide have been made with this process [67].

Research involving the 3DP of ceramics encountered early setbacks because of the use of dry powders. The fine powders needed for good powder bed density did not generally flow well enough to spread into defect-free layers [66]. Furthermore, since green part density was inadequate with the use of dry powders, isostatic pressing was implemented after the printing process. This extraneous requirement severely limits the types of part shapes capable of being processed.

To counteract the problems encountered with recoating a dry powder bed, research on ceramic 3DP has shifted to the use of a slurry-based working material. In this approach, layers are first deposited by ink-jet printing a layer of slurry over the build area. After the slurry dries, binder is selectively printed to define the part shape. This is repeated for each individual layer, at the cost of significantly increased build time. Multiple jets containing different material composition or concentration could be employed to prepare components with composition and density variation on a fine scale (100 μm) [68]. Alumina and silicon nitride have been processed with this technique, improving green part density to 67%, and utilizing layer thicknesses as small as 10 μm [69].

Recently, a variation of this method was developed to fabricate metal parts starting with metal-oxide powders [70]. The ceramic 3DP is used until the furnace sintering step. While in the furnace, a hydrogen atmosphere is introduced, causing a reduction reaction to occur between the hydrogen and the oxygen atoms in the metal-oxide. The reduction reaction converts the oxide to metal. After reduction, the metal particles are sintered to form a metal part. This process has been demonstrated for several material systems, including iron, steels, and copper. Unfortunately, reaction thermodynamics prevent alumina and titanium oxide from being reduced to aluminum and titanium, respectively.

This Metal-Oxide Reduction 3DP (MO3DP) process was demonstrated using a Z405 machine [71]. Metal oxide powders containing iron oxide, chromium oxide, and a small amount of molybdenum were prepared by spray drying the powder composition with polyvinyl alcohol (PVA) to form clusters of powder particles coated with PVA. Upon reduction, the material composition formed a maraging steel. Water was selectively printed into the powder bed to define part cross sections, since the water will dissolve PVA, causing the clusters to stick together. A variety of shapes (trusses, channels, thin walls) were fabricated using the process to demonstrate the feasibility of producing cellular materials.

The main advantage of 3DP, in the context of manufacturing cellular materials, lies in its economic considerations. Simply put, the 3DP process does not require high energy, does not involve lasers or any toxic materials, and is relatively inexpensive and fast. Part creation rate is limited to approximately twice the binder flow rate. A typical inkjet nozzle delivers approximately 1 cm^3/min of binder; thus a machine with a 100 nozzle printhead could create up to approximately 200 cm^3/min of printed component. Because commercial inkjet printers exist with up to 1,600 nozzles, 3DP could be fast enough to be used as a production process.

7.7 Advantages of Binder Printing

The binder printing processes share many of the advantages of direct printing relative to other AM processes. With respect to direct printing, binder printing has some distinct advantages. First, it can be faster since only a small fraction of the total part volume must be dispensed through the print heads. However, the need to recoat powder adds an extra step, slowing down binder processes somewhat. Second, the combination of powder materials and additives in binders enables material compositions that are not possible, or not easily achieved, using direct methods. Third, slurries with higher solids loadings are possible with binder printing, compared with direct printing, enabling better quality ceramic and metal parts to be produced. As mentioned earlier, binder printing processes lend themselves readily to printing colors onto parts.

As a general rule, however, parts fabricated using binder printing processes tend to have poorer accuracies and surface finishes than parts made with direct printing. Infiltration steps are needed to fabricate dense parts or to ensure good mechanical properties.

As with any set of manufacturing processes, the choice of manufacturing process and material depends largely on the requirements of the part or device. It is a matter of compromising on the best match between process capabilities and design requirements.

7.8 Exercises

1. Explain why support structures are not needed in the 3DP process.
2. List five types of material that can be directly printed.
3. According to the printing indicator (7.7), what is the smallest diameter nozzle that could be used to print a ceramic-wax material that has the following properties:
   (a) Viscosity of 15 cP, density of 1,800 kg/m^3, and surface tension of 0.025 N/m.
   (b) Viscosity of 7 cP, density of 1,500 kg/m^3, and surface tension of 0.025 N/m.
   (c) Viscosity of 38 cP, density of 2,100 kg/m^3, and surface tension of 0.025 N/m.
4. Develop a build time model for a printing machine. Assume that the part platform is to be filled with parts and the platform is L mm long and W mm wide. The printhead width is H mm. Assume that a layer requires three passes of the printhead, the printhead can print in both directions of travel ($+X$ and $-Y$), and the layer thickness is T mm. Figure 7.17 shows a schematic for the problem. Assume that a delay of D seconds is required for cleaning the printheads every K layers. The height of the parts to be printed is P mm.
   (a) Develop a build time model using the variables listed in the problem statement.

Compute the build time for a layer of parts given the variable values in the following table.

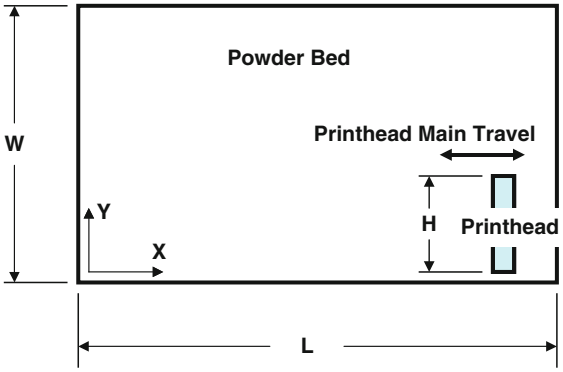

Fig. 7.17 Schematic for problems 4–5

	L	W	H	T	D	K	P
(b)	300	185	50	0.04	10	20	60
(c)	300	185	50	0.028	12	25	85
(d)	260	250	60	0.015	12	25	60
(e)	340	340	60	0.015	12	25	60
(f)	490	390	60	0.015	12	25	80

5. Modify the build time model from Problem 4 for the 3DP process. Assume that the powder bed recoating time is 10 s. Compute build times for a layer of parts using the values in Problem 4, assuming that layer thicknesses are 0.1 mm.
6. The integral in (7.2) can be evaluated analytically for simple nozzle shapes. Assume that the nozzle is conical with the entrance diameter of d_e and the exit diameter d_x.
   (a) evaluate the integral analytically.

Use your integrated expression to compute pressure drop through the nozzle, instead of (7.3), for the following variable values:

	d_e [mm]	d_x [mm]	l [mm]	μ [cP]	ρ [kg/m^3]	γ [N/m]	v [m/s]
(b)	0.04	0.02	0.1	1	1,000	0.072	10
(c)	0.04	0.02	0.1	40	1,000	0.072	10
(d)	0.04	0.02	1.0	1	1,000	0.072	10
(e)	0.1	0.04	5.0	1	1,000	0.072	10
(f)	0.1	0.04	5.0	40	1,000	0.025	10

7. Using the integral from Problem 6, develop a computer program to compute pressure drop through the nozzle for various nozzle sizes and fluid properties. Compute and plot the pressure drop for the printing conditions of Fig. 7.14, but using nozzles of the following dimensions:

(a) $l = 0.1$ mm, $d_e = 0.06$ mm, $d_x = 0.02$ mm

(b) $l = 0.1$ mm, $d_e = 0.08$ mm, $d_x = 0.04$ mm
(c) $l = 0.1$ mm, $d_e = 0.12$ mm, $d_x = 0.05$ mm
(d) $l = 5.0$ mm, $d_e = 0.1$ mm, $d_x = 0.05$ mm

References

1. Le HP (1998) Progress and trends in ink-jet printing technology. J Imaging Sci Technol 42(1):49–62
2. The rapid prototyping patent museum: basic technology patents. http://home.att.net/~rppat/museum/mus_2.htm. Accessed 19 March 2006
3. Wohlers T (2004) Wohlers Report 2004. Wohlers Associates, Fort Collins
4. Solidscape. T66 Benchtop: Product Description. http://www.solid-scape.com/t66.html. Accessed 31 July 2006
5. Polyjet technology – 3-dimensional printing applications. http://www.2objet.com. Accessed 19 March 2006
6. In-Vision 3D printer. http://www.cadem.com.tr/3dsystems/invision/index.html. Accessed 19 March 2006
7. Gao F, Sonin AA (1994) Precise deposition of molten microdrops: the physics of digital fabrication. Proc R Soc Lond A 444:533–554
8. Reis N, Seerden KAM, Derby B, Halloran JW, Evans JRG (1999) Direct inkjet deposition of ceramic green bodies: II – jet behaviour and deposit formation. Mater Res Soc Symp Proc 542:147–152
9. Feng W, Fuh J, Wong Y (2006) Development of a drop-on-demand micro dispensing system. Materials Science Forum 505–507 (January 2006):25–30
10. Tay B, Edirisinghe MJ (2001) Investigation of some phenomena occurring during continuous ink-jet printing of ceramics. J Mater Res 16(2):373–384
11. Derby B, Reis N (2003) Inkjet printing of highly loaded particulate suspensions. MRS Bull 28(11):815–818
12. Ainsley C, Reis N, Derby B (2002) Freeform fabrication by controlled droplet deposition of powder filled melts. J Mater Sci 37:3155–3161
13. Zhao X, Evans JRG, Edirisinghe MJ (2002) Direct ink-jet printing of vertical walls. J Am Ceram Soc 85(8):2113–2115
14. Wang T, Derby B (2005) Ink-jet printing and sintering of PZT. J Am Ceram Soc 88(8): 2053–2058
15. Liu Q, Orme M (2001) High precision solder droplet printing technology and the state-of-the-art. J Mater Process Technol 115:271–283
16. Priest JW, Smith C, DuBois P (1997) Liquid metal jetting for printing metal parts. Solid Freeform Fabrication Symposium
17. Orme M (1993) A novel technique of rapid solidification net-form material synthesis. J Mater Eng Perform 2:399–405
18. Orme M, Huang C, Courter J (1996) Precision droplet-based manufacturing and material synthesis: fluid dynamics and thermal control issues. Atomization and Sprays 6:305–329
19. Yamaguchi K (2003) Generation of 3-dimensional microstructure by metal jet. Microsystem Technol 9:215–219
20. Yamaguchi K, Sakai K, Yamanka T, Hirayama T (2000) Generation of three-dimensional micro structure using metal jet. Precision Eng 24:2–8
21. Liu Q, Orme M (2001) On precision droplet-based net-form manufacturing technology. Proc I MECH E Part B – J Eng Manufacture 215:1333–1355
22. Cao W, Miyamoto Y (2006) Freeform fabrication of aluminum parts by direct deposition of molten aluminum. J Mater Process Technol 173:209–212

23. Furbank RJ, Morris JF (2004) An experimental study of particle effects on drop formation. Phys Fluids 16(5):1777–1790
24. Bechtel SE, Bogy DB, Talke FE (1981) Impact of a liquid drop against a flat surface. IBM J Res Dev 25(6):963–971
25. Pasandideh-Fard M, Qiao Y, Chandra S, Mostaghimi J (1996) Capillary effects during droplet impact on a solid surface. Phys Fluids 8(3):650–659
26. Thoroddsen ST, Sakakibara J (1998) Evolution of the fingering pattern of an impacting drop. Phys Fluids 10(6):1359–1374
27. Bhola R, Chandra S (1999) Parameters controlling solidification of molten wax droplets falling on a solid surface. J Mater Sci 34:4883–4894
28. Attinger D, Zhao Z, Poulikakos D (2000) An experimental study of molten microdroplet surface deposition and solidification: transient behavior and wetting angle dynamics. J Heat Transf 122:544–556
29. Bussman M, Chandra S, Mostaghimi J (2000) Modeling the splash of a droplet impacting a solid surface. Phys Fluids 12(12):3121–3132
30. Schiaffino S, Sonin AA (1997) Molten droplet deposition and solidification at low Weber numbers. Phys Fluids 9(11):3172–3187
31. Orme M, Huang C (1997) Phase change manipulation for droplet-based solid freeform fabrication. J Heat Transf 119:818–823
32. Sanders R, Forsyth L, Philbrook K (1996) 3-D Model maker. US Patent No. 5506706
33. Thayer J, Almquist T, Merot C, Bedal B, Leyden R, Denison K, Stockwell J, Caruso A, Lockard M (2001) Selective deposition modeling system and method. US Patent No. 6305769
34. Gothait H (2005) System and method for three-dimensional model printing. US Patent No. 6850334
35. Gothait H (2001) Apparatus and method for three-dimensional model printing. US Patent No. 6259962
36. Bedal B, Bui V (2002) Method and apparatus for controlling the drop volume in a selective deposition modeling environment. US Patent No. 6347257
37. Tay B, Evans JRG, Edirisinghe MJ (2003) Solid freeform fabrication of ceramics. Int Mater Rev 48(6):341–370
38. De Gans BJ, Duineveld PC, Schubert US (2004) Inkjet printing of polymers: state of the art and future developments. Adv Mater 16(3):203–213
39. MicroFab technote 99-01: Background on ink-jet technology. http://www.microfab.com/equipment/technotes/technote99-01.pdf. Accessed 19 March 2006
40. Teng W, Edirisinghe MJ (1998) Development of continuous direct ink jet printing of ceramics. Br Ceram Trans 97(4):169–173
41. Blazdell PF, Evans JRG, Edirisinghe MJ, Shaw P, Binstead M (1995) The computer aided manufacture of ceramics using multilayer jet printing. J Mater Sci Lett 54:1562–1565
42. Blazdell PF (2003) Solid free-forming of ceramics using a continuous jet printer. J Mater Process Technol 137:49–54
43. Tseng AA, Lee MH, Zhao B (2001) Design and operation of a droplet deposition system for freeform fabrication of metal parts. J Eng Mater Technol 123:74–84
44. Basaran OA (2002) Small-scale free surface flows with breakup: drop formation and emerging applications. AIChE J 48(9):1842–1848
45. Sirringhaus H, Kawase T, Friend RH, Shimoda T, Inbasekaran M, Wu W, Woo EP (2000) High-resolution inkjet printing of all-polymer transistor circuits. Science 290:2123–2126
46. Shimoda T, Morii K, Seki S, Kiguchi H (2003) Inkjet printing of light-emitting polymer displays. MRS Bull 28:821–827
47. Lee E (2002) Microdrop generation. CRC Press, Boca Raton
48. Percin G, Khuri-Yakub BT (2002) Piezoelectrically actuated flextensional micromachined ultrasound droplet ejectors. IEEE Trans Ultrason Ferroelectr Freq Control 49(6):756–766

49. Elrod SA, Hadimioglu B, Khuri-Yakub BT, Rawson EG, Richley E, Quate CF (1989) Nozzleless droplet formation with focused acoustic beams. J Appl Phys 65(9):3441–3447
50. Meacham JM, Ejimofor C, Kumar S, Degertekin FL, Fedorov AG (2004) Micromachined ultrasonic droplet generator based on a liquid horn structure. Rev Sci Instrum 75(5):1347–1352
51. Meacham JM, Varady M, Degertekin FL, Fedorov AG (2005) Droplet formation and ejection from a micromachined ultrasonic droplet generator: visualization and scaling. Phys Fluids 17:100605
52. Margolin L (2006) Ultrasonic droplet generation jetting technology for additive manufacturing: an initial investigation. MS Thesis, Georgia Institute of Technology
53. Fukumoto H, Aizawa J, Nakagawa H, Narumiya H (2000) Printing with ink mist ejected by ultrasonic waves. J Imaging Sci Technol 44(5):398–405
54. Sweet R (1964) High-frequency oscillography with electrostatically deflected ink jets. SEL-64-004, SELTR17221. Stanford Electronics Laboratories, Stanford, California
55. Munson B, Young D, Okiishi T (1998) Fundamentals of fluid mechanics, 3rd edn. Wiley, New York
56. MicroFab Technologies. MicroFab technote 99-02: fluid properties effects on ink-jet device performance. http://www.microfab.com/equipment/technotes.html
57. De Gans BJ, Kazancioglu E, Meyer W, Schubert US (2004) Ink-jet printing polymers and polymer libraries using micropipettes. Macromol Rapid Commun 25:292–296
58. Paton A, Kruse J (1995) Reduced nozzle viscous impedance. US Patent No. 5463416.
59. Leyden R, Hull W (1999) Method for selective deposition modeling. US Patent No. 5855836
60. Orme M, Courter J, Liu Q, Huang C, Smith R (2000) Electrostatic charging and deflection of nonconventional droplet streams formed from capillary stream breakup. Phys Fluids 12(9):2224–2235
61. Zhao X, Evans JRG, Edirisinghe MJ, Song JH (2001) Ceramic freeforming using an advanced multinozzle ink-jet printer. J Mater Synth Process 9(6):319–327
62. Xu P, Ruatta S, Schmidt K, Doan V (2004) Phase change support material composition. US Patent No. 66
63. Schmidt K (2005) Selective deposition modeling with curable phase change materials. US Patent No. 6841116
64. Sachs EM, Cima MJ, Williams P, Brancazio D, Cornie J (1992) Three-dimensional printing: rapid tooling and prototypes directly from a CAD model. J Eng Ind 114:481–488
65. Ex One, www.exone.com
66. Yoo J, Cima MJ, Khanuja S, Sachs EM (1993) Structural ceramic components by 3D printing. Solid freeform fabrication symposium, Austin, TX
67. Uhland S, Holman RK, Morissette S, Cima MJ, Sachs EM (2001) Strength of green ceramics with low binder content. J Am Ceram Soc 84(12):2809–2818
68. Cima MJ, Lauder A, Khanuja S, Sachs E (1992) Microstructural elements of components derived from 3D printing. Solid freeform fabrication symposium, Austin, TX
69. Grau J, Moon J, Uhland S, Cima MJ, Sachs E (1997) High green density ceramic components fabricated by the slurry-based 3DP process. Solid freeform fabrication symposium, Austin, TX
70. Williams CB, Rosen DW (2007) Cellular materials manufactured via 3D printing of metal oxide powders. Solid freeform fabrication symposium, Austin, TX, 6–8 Aug 2007
71. Williams CB (2008) Design and development of a layer-based additive manufacturing process for the realization of metal parts of designed mesostructure. Ph.D. Dissertation, Georgia Institute of Technology
72. Wohlers T (2006) Wohlers Report 2006. Wohlers Associates, Fort Collins, CO
73. Rapid prototyping: Let it grow. http://deskeng.com/articles/03/may/resourceguide/chart.pdf. Accessed 31 July 2006
74. Turkcadcam.net. http://www.turkcadcam.net/rapor/otoinsa/tek-harc-yigma-puskurterek.html. Accessed 31 July 2006

75. Desktop Engineering Magazine. Three printers: Same parts, different results. http://www.deskeng.com/Articles/Hardware-Review/Three-Printers:-Same-Parts,-Different-Results-20051216783.html. Accessed 31 July 2006
76. Engineer Live. 3D printing reaches out to the desktop and workshops of engineers and designers. http://www.engineerlive.com/homepage/features/14943/3d-printing-reaches-out-to-the-desktops-and-workshops-of-engineers-and-designers.thtml. Accessed 22 July 2006